

ACTIVE SPACECRAFT POTENTIAL CONTROL - AN ION EMITTER EXPERIMENT

W. Riedler

Institut für Weltraumforschung der Österreichischen Akademie der Wissenschaften
Inffeldgasse 12, A-8010 Graz, Austria

R. Goldstein

Jet Propulsion Laboratory, Pasadena, CA 91109,
U.S.A.

M. Hamelin

Laboratoire de Physique et Chimie de
l'Environnement, CNRS, F-45045 Orleans, France

B.N. Maehlum and J. Trøim

Forsvarets Forskningsinstitutt, N-2007 Kjeller,
Norway

R.C. Olsen

Naval Postgraduate School, Monterey, CA 93943,
U.S.A.A. Pedersen, R.J.L. Grard, R. Schmidt
Space Science Department, ESA/ESTEC, NL-2200
AG Noordwijk, The Netherlands

F. Rüdener and W. Steiger

Österreichisches Forschungszentrum Seibersdorf,
A-2444 Seibersdorf, Austria

R. Torbert

The University of Alabama, Huntsville, AL 35899,
U.S.A.

K.M. Torkar

Institut für Weltraumforschung der ÖAW, A-8010
Graz, Austria

N. Valavanoglou

Technische Universität Graz, A-8010 Graz, Austria

E. Whipple

University of California at San Diego, La Jolla,
CA 92093, U.S.A.**ABSTRACT**

Charging of the outer surface or entire structure of a spacecraft in orbit can have a severe impact on the scientific output of the instruments. Typical floating potentials for magnetospheric satellites (from +1 to +50 V in sunlight) make it practically impossible to measure the very cold component of the ambient plasma. The Cluster spacecraft will be instrumented with ion emitters for charge neutralisation. The emitters will produce Indium ions at approximately 6 keV. The ion current will be adjusted in a feedback loop with instruments measuring the spacecraft potential (EFW and PEACE). A stand-alone mode is also foreseen as a backup.

The design of the active spacecraft potential control instrument (ASPOC), especially of the ion emitters, is presented in detail. The operating principle is field evaporation of Indium in the apex field of a needle. The advantages are low power consumption, compactness, and high mass efficiency.

Keywords: Potential Control, Spacecraft Potential, Active Experiment, Ion Emitter, Ion Beam, Indium

1. INTRODUCTION

Spacecraft in the Earth's magnetosphere and in the solar wind environment charge electrostatically in response to various charging currents. The most important currents are due to photo-emission caused by sunlight, plasma currents due to the environmental electrons and ions, and secondary electron currents caused by the impact of primary electrons and ions. In steady state a spacecraft will charge to an equilibrium potential where the sum of the currents vanish so that there is no net transfer of charge between the spacecraft and the environment. (See Refs. 1-2 for reviews.)

In the Earth's ionosphere and plasmasphere where the plasma densities are relatively high, the dominant currents are the plasma ion and electron currents. Spacecraft in these regions charge to negative potentials of a few volts because of the lower mass and consequently higher thermal velocities of the electrons as compared to the ions. Outside the plasmasphere where the plasma density is low, and as long as the electron temperature is not too high (less than a few keV), current balance to a spacecraft is usually between the plasma electron current and photo-emission, and spacecraft potentials are a few volts positive. In extremely low density plasmas such as in the

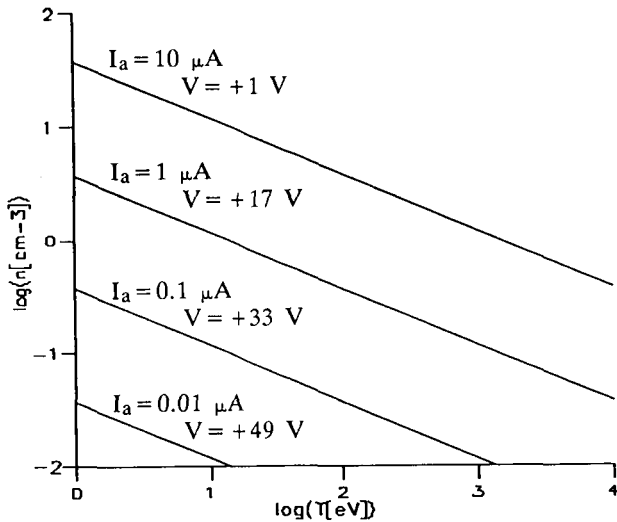


Figure 1. Contours of calculated spacecraft potential as function of ambient plasma parameters.

lobes of the Earth's magnetotail, potentials can be as high as +50 V and more. GEOS and ISEE observations for sunlight have been summarised in Ref. 3 (Table 1).

Because of the conductive surface of a Cluster spacecraft its potential should be similar to that of the GEOS and ISEE S/C: namely, the potential should be determined by a balance between photo-emission and plasma electrons as long as the S/C is outside the plasmasphere and in sunlight. Refs. 4-5 have shown for GEOS-2, and Lindqvist (Ref. 6) has shown for ISEE-1 that the potentials for these S/C were determined by the quantity $(n \sqrt{T})$, where n is the plasma electron density, and T the electron temperature. The plasma electron current to these S/C is also nearly proportional to this quantity. If we use the ISEE-1 value for photo-electron current (0.5 nA cm^{-2}) and 10 m^2 for a Cluster S/C area (so the photo-electron emission is about 5 μA), then numerical values of the plasma electron current from the ambient plasma (I_a) to and potential of a Cluster S/C (V) are obtained by:

$$I_a = 2.7 \cdot 10^{-7} n \sqrt{T} \quad [\text{A}] \quad (1)$$

$$V = 27.2 - 7 \ln(n \sqrt{T}) \quad [\text{V}] \quad (2)$$

where n is in electrons/cm^3 and T in eV . These relations are shown in Fig. 1 which has contours of constant potential and constant plasma electron current as a function of electron density and electron temperature. Schmidt and Pedersen (Ref. 5) have suggested somewhat higher values for photo-electron current. If we use a value of 5 nA cm^{-2} , then the equilibrium potentials must all be increased by 16 V.

2. SCIENTIFIC OBJECTIVES AND CAPABILITIES

2.1 Reasons for Satellite Charge Control

The primary motivation for active spacecraft potential control (ASPOC) is to insure effective, complete measurement of the ambient plasma distribution functions. Additional benefits may be found in improved data for the long wire electric field measurement, and the electron beam probe for electric fields.

Typical floating potentials for magnetospheric satellites of up to +50 V obscure, or render impossible the measurement of the core of the ion distribution function, which has a thermal energy comparable to

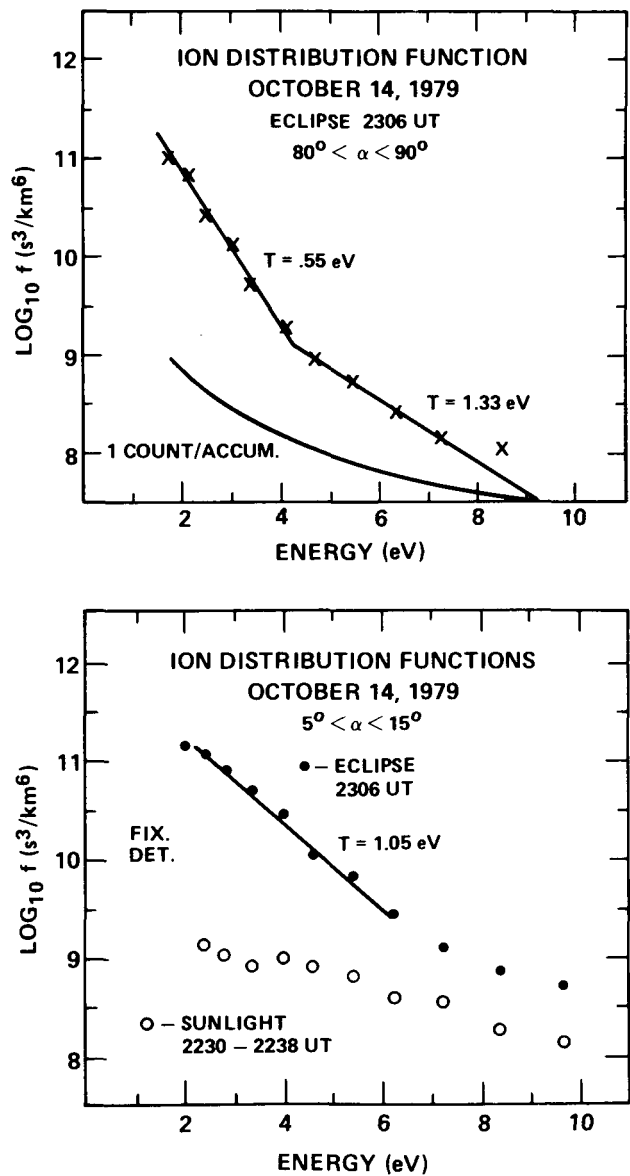


Figure 2. Data from the SCATHA satellite, in sunlight and eclipse, at local midnight, near geosynchronous orbit.

the satellite potential. This problem was indicated by discrepancies in density calculations from satellites such as GEOS-1 (Ref. 7). The densities inferred from ion spectrometers, for example, did not agree with the total electron density measurements obtained from wave techniques. Measurements in eclipse, made on ATS-6, SCATHA, and DE-1 have shown the appearance of previously 'hidden' ion populations, invisible in sunlight (Ref. 8).

Figure 2, from Ref. 8, shows ion distribution functions for the outer plasmasphere. The 90 degree measurements (upper panel) show the low temperature plasma visible in an eclipse. The field-aligned component (lower panel) shows how deceptive the sunlight measurements can be — the high energy tail has a different temperature than the core of the plasma distribution. These unique measurements of the outer plasmasphere, at the equator, were possible only because the absence of the photo-current allowed the satellite potential to fall to near 0 V. Unfortunately, this situation is a rather rare occurrence, since it is only possible at local midnight, in the near-Earth regions.

Other fundamental problems occur in the measurement of the anisotropic distributions outside the plasmasphere, such as the field aligned flows which make up the polar wind (Ref. 9). The bulk of the distribution is lost due to the satellite potential, and it is not possible to obtain fundamental parameters such as density, temperature, and flow velocity for H^+ . Such flows have been observed at the inner edge of the plasma sheet, at the equator, during an eclipse on one occasion (Ref. 10), when the S/C potential was near zero.

Also electron measurements gain by satellite potential control: Usually, the low energy portion of the electron spectra is contaminated by photo-electrons from the satellite surface, trapped by the positive satellite potential. Such effects can cause substantial errors in interpreting electron spectra, as illustrated by Ref. 1 in their critique of Jovian measurements of low energy electrons. The ambient distribution is distorted by the satellite sheath, so that high order moments of the distribution function are not determined correctly. Automatic calculation of these moments, in particular, is made more difficult. For example, Ref. 12 used moment techniques to analyse solar wind and Jovian plasma data. Their analysis required substantial work to obtain the satellite I-V characteristic, firstly to obtain the satellite potential, and secondly to correct for the effect. Even then, their magnetospheric (Jovian) moment calculations were questionable, because the calibration technique used solar wind plasmas, which differ in temperature, and hence secondary production, from the magnetosphere plasmas.

Deleterious effects of S/C charging also extend to electric field measurements. The double probe technique for electric field measurements can respond to the local electric field induced by the satellite charge. This is one motivation for extending the booms to

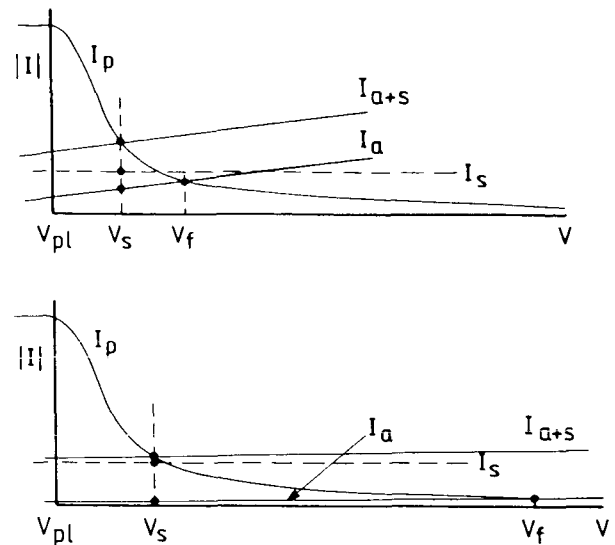


Figure 3. Representative spacecraft I-V characteristics, showing effect of active ion emission on S/C potential.

substantial distances from the satellite. By reducing the positive potential of the satellite and on the conductive long wire booms, supporting the electric field probes, the local field perturbation should be reduced, enhancing the electric field measurement.

The electron beam technique for electric field measurements is also somewhat sensitive to satellite potential. If the beam energy is 1 keV and the S/C potential is 10 V, the perturbation to the measurement is about 1%. The disturbance should be kept to low values in order to be able to use the full capability of the beam technique to measure small electric fields.

2.2 Technique of Spacecraft Potential Control

The basic approach to the active control of spacecraft potential involves the emission of charges from the S/C sufficient to balance the excess of charge accumulating on the vehicle from the environment. For the case of primary concern here, where photo-emission of electrons drives the S/C potential positive relative to the plasma potential, it is necessary to emit positive ions. One approach to the technique has, for example, been described in Ref. 3. This is illustrated by reference to Fig. 3. In the upper portion (a) the normal floating potential, indicated by " V_f ", occurs where the photo-electrically emitted current equals the collected current from the ambient plasma (as shown above). If additional positive current (I_{s+}) is emitted, this can be represented in the Figure by shifting the ambient current curve by an amount equal to I_s (assumed to be constant). Such a curve is shown in the Figure and labelled " I_{a+s} ".

The intersection with the photo-emission curve occurs at a lower potential (V_s); hence this arrangement reduces the floating potential of the S/C. By adjusting the positive emission current, the spacecraft potential

can thus be adjusted to near zero. Under other ambient plasma conditions, say a more tenuous plasma as in Fig. 3b, the normal floating potential V_f would be greater than in the previous case.

Again, a curve " I_{a+s} " shows the effect of positive ion emission on reducing the S/C potential. In this case, a slightly higher emission current would be needed to bring the S/C potential to the same value as the case in Fig. 3a.

2.3 Operational Modes

At the heart of the system for active control of the S/C potential is a device which emits a constant, but adjustable current of In^+ ions. The device itself is discussed in detail below. Here we describe how the device is used for potential control.

There are two basic operation modes. In one mode a measurement of the S/C potential is supplied to ASPOC by either the electric field experiment (EFW) or the electron analyser (PEACE) and this information is then used to adjust the emission current sufficient to reduce the S/C potential to within some predetermined value, as described in the discussion of Fig. 3. Referring to Fig. 1, we see that over most of the plasma regime of interest, photo-emission dominates the current balance to the spacecraft, and the required ion emission current to control the S/C potential would be the order of a few tens of mA. In the case of plasma current domination, the required emission current would be smaller.

The amount of current is determined by the on-board stored knowledge of the I-V characteristics of the spacecraft. From a considerable amount of previous experience (Refs. 4-6), the I-V characteristics of typical S/C are already well-known. But we also foresee the necessity for a measurement of this characteristic for each Cluster S/C at the beginning of the mission, and occasionally a re-measurement to account for changes in the photo-emission properties of the surface. (This measurement is simply carried out by measuring S/C potential as function of ion emission current, over some convenient range.) Note that it is also possible to obtain information on the S/C potential from the low energy plasma experiments, if these experiments perform appropriate on-board processing of their data.

Apart from providing a highly improved environment for other experiments, scientific investigations of the photoelectric characteristics, dependence of the S/C potential on plasma parameters, and of S/C charging in different plasma environments can be carried out in this mode. In accordance with the scientific community the optimum ion current can be varied in a defined way for a short time to enable the co-operating plasma experiments to calibrate their response to S/C potential variations between the unregulated and the clamped, near-zero values.

In case no signal from EFW or PEACE is available, a second mode of operation involves setting the emission current to some predetermined value based on the S/C I-V characteristics, and perhaps a measure of the ambient plasma density and temperature. In this mode, the emission current must be set to a level to insure that the S/C potential is not driven negative. The control of potential would not be as good in this case as in the first mode described, but could still be used to reduce the S/C potential to a few volts positive relative to the ambient plasma potential.

2.4 Precautions Against Interference With Other Experiments

2.4.1 Electromagnetic Compatibility and Beam/Spacecraft Interaction. Any harmful effect on any other experiment by actively controlling the S/C potential is unlikely if the emission current is kept within reasonable limits. However, the necessity of operating the emitter in close consultation with all the other experimenters is acknowledged.

The emission of a charged particle beam into a plasma is a potential source of electromagnetic noise. The extent of this possibility for the case of ASPOC is not yet well understood, especially since a dedicated active potential control experiment using an ion beam has not yet been operated on a spacecraft. A first attempt will be undertaken on the Soviet Interball mission planned to be launched in 1990 (Ref. 13). This instrument basically includes the same liquid metal ion source and its routine operation is expected to shed more light on the understanding of the beam-plasma interaction.

Theoretical work on the triggering of activity by beams with current densities as low as in the proposed experiment and at 6 keV is practically non-existent in the literature. Ion beams with two orders of magnitude higher current densities were injected into the ionosphere and generated waves around the lower hybrid resonance frequency. Other experiments found increased emission in the magnetic field around the local electron gyrofrequency. In this case the electric field antenna did not measure any effect.

It is known that a small opening angle of a beam tends to increase the probability of wave generation. For this reason the beam focusing system is designed for a large opening angle of 15° half width.

2.4.2 Chemical Contamination by the Ion Beam. Chemical interaction that could be considered as potential concerns to the spacecraft or instruments covers:

- Condensation of neutral Indium in the vicinity of the ion emitter,
- Return to the spacecraft of In^+ ions after one or more gyrations,
- Interaction of the ion beam with S/C surfaces.

The condensation of neutral Indium on cold surfaces is extremely unlikely. The vapour pressure of Indium is only $1.1 \cdot 10^{-19}$ Torr at the melting point and the total surface from which Indium evaporates is in the order of 1 mm^2 for the active, hot emitter and about 9 mm^2 for the surfaces at the environmental temperature. Furthermore, a baffle is provided by the beam focusing electrodes together with the box orifice. Neutrals that penetrate through the orifice are expected to drift freely into the ambient plasma. Their return to the S/C skin can only occur through two unlikely processes: the first possibility is that due to collisions the path of the neutrals is reflected back towards the spacecraft. The typical mean free path length is of the order of $>1000 \text{ m}$ if the spacecraft generated atmosphere in its close vicinity was a bad 10^{-6} Torr; it would be in excess of 10^6 m if the pressure dropped below 10^{-8} Torr. Hence, collisions are extremely unlikely to occur. Another possibility would be introduced by photo-ionisation of Indium and attraction of these ions by negatively charged, non-conductive and shadowed surfaces. The photo-ionisation efficiency at 1 AU is in the order of 10^{-7} . The particle density, inferred from the Indium partial pressure of 10^{-15} Torr at nominal operating temperature, is $n = 10^3 \text{ m}^{-3}$, which yields a negligible amount of In^+ to be produced in the neighbourhood of the S/C. A condensation of Indium, even after lengthy laboratory tests was never found inside the vacuum tank.

The return of the In^+ beam to the spacecraft can be assessed in the following way. The typical ion energy will be about 6 keV. Ions come back to the S/C whenever the beam injection takes place about perpendicular to the ambient magnetic field. In the Cluster orbit the magnetic field encountered in the near-perigee and -apogee segments of the orbit will reach respectively about 1000 nT and 10 nT. This yields for the Indium gyration period, s , and radius, R_G :

	s [sec]	R_G [km]	B [nT]
perigee	7.5	120	1000
apogee	750	12000	10

2.4.3 Negative S/C Potential Problems. There are two basic constraints for active ion beam emission. It is not possible to operate the instrument at total pressures $>3 \cdot 10^{-6}$ Torr for extended time periods (>1 hour). When the uncontrolled S/C potential is negative with respect to the ambient plasma routine operation of ASPOC is not foreseen to avoid driving the S/C potential more negative.

Only the latter condition is relevant for the Cluster orbit. In feed-back mode the onboard software of the instrument will switch off the ion beam. In stand-alone mode the beam current is set to a pre-determined value derived from theoretical considerations and preceding in-flight tests. This value can be pre-programmed to vary according to the expected plasma environment along the trajectory including a safety margin to avoid beam-induced negative charging under abnormal conditions.

From an operational point of view negative charging is expected to occur in the following orbital phases:

- eclipse
- radiation belt crossing
- plasma density higher than 1000 cm^{-3} : plasma-sphere and near-perigee parts of the orbit

3. TECHNICAL SOLUTION

3.1 Liquid Metal Ion Source (LMIS)

3.1.1 Operating Principle. The ion emitter is a "solid needle" - type liquid metal ion source, previously described in the literature using Indium as charge material (Refs. 14-17). A solid needle, usually made of Tungsten (W), with a tip radius between 2 and $15 \mu\text{m}$ is mounted in a heated reservoir with the charge material (Fig. 4). A potential of 5 - 10 kV is applied between the needle and an extractor electrode. If the needle is well wetted by the metal, the electrostatic stress at the needle tip pulls the liquid metal towards the extractor electrode. This stress is counteracted by the surface tension forces of the liquid. One of the equilibrium configurations the liquid surface can assume is that of a Taylor-cone (Ref. 18) with a total tip angle of 98.6° . The apex of the Taylor-cone in practice reaches a diameter of 1 to 5 nm (Ref. 19). The field evaporation of positively charged metal atoms in the strong apex field leads to emission of a high brightness external ion beam from this cone apex with a beam brightness of the order of $10^6 \text{ A cm}^{-2} \text{ sr}^{-1}$ at 10 keV beam energy.

Since the emission zone is in the liquid state, ions leaving the surface can be continuously replenished by hydrodynamic flow of liquid metal from the reservoir to the needle apex so that a stable emission can be maintained.

Due to the extremely high source brightness, the LMIS is particularly suited for formation of microfo-

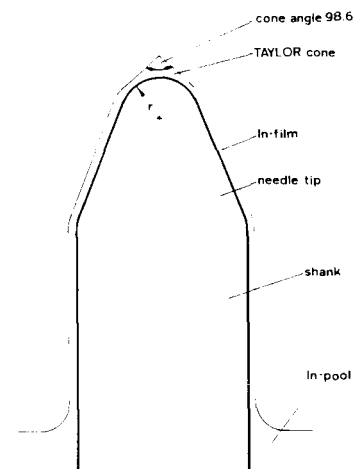


Figure 4. Solid needle type liquid metal ion source (LMIS), schematic.

cused ion beams and has found wide application in microelectronic technology: ion beam lithography, writing ion implantation (Ref. 20), ion microfabrication (Ref. 21) and microanalysis (Ref. 22). The

basic technology is well developed on an industrial basis. Past space applications, however, have not been reported with exception of laboratory development of a field emission electrical propulsion system (FEPEP; Ref. 23). The advantages of the LMIS principle are:

- low power consumption; mostly determined by the heater power to keep the Indium reservoir above 429 K;
- high mass efficiency;
- compactness and low mass; one individual emitter has a volume of 170 mm^3 and a mass $< 5.2 \text{ g}$.

Indium is chosen as ion source charge material because of its low vapour pressure. This prevents contamination of the source insulators and ambient S/C surfaces. On the other hand, the melting point is high enough that melting of an unheated source charge cannot occur even at the maximum expected elevated environmental temperature.

Laboratory tests (Ref. 24) revealed that the dominant emission component is the singly charged Indium species (115 AMU) with minor contributions from singly and doubly charged Indium clusters. According to measured spectra, the average charge number per emitted charged Indium atom is 0.976. At an emission current of $10 \mu\text{A}$, the energy width is 150 eV, but a low intensity, low energy tail down to more than 500 eV below nominal beam energy can be expected.

3.1.2 Design of Emitter Module. Figure 5a shows the schematic design of an ion emitter module. One such module consists of an array of 5 individual ion emitters which are operated one at a time. The individual emitters (Fig. 5b) are of cylindrical geometry (1). The Indium and the needle (2) are kept at high tension (HT) by the HT supply (3). The LMIS's are individually and indirectly heated by a thick film resistor embedded into a ceramic insulator tube. Al_2O_3 (4),(5) was chosen for superior high voltage insulation characteristics. This scheme enables the source to be heated from a grounded power supply (6) and the tip itself still being kept at the HT. The individual emitters are mounted in a slab of porous ceramic (7) with extremely low heat conduction ($< 5 \cdot 10^{-4} \text{ W K}^{-1} \text{ cm}^{-1}$). All emitters have a common extraction- and focusing lens arrangement consisting of a grounded extractor electrode (8), a focusing electrode (9) at beam potential and a second ground electrode (10). The three electrodes (8)-(10) constitute a unipotential lens with the tip apex located in one focal point. The divergent ion beam (opening angle $\approx 30^\circ$) emitted from the tip is focused by this lens into a nominally parallel beam after passage through the ground electrode (10). All outer surface grounds (14) will be connected to S/C chassis ground. The cold secondary side of the HT supply, which is connected to the inner shield (12) and focusing system (8,10) inside the emitter housing, will be floating.

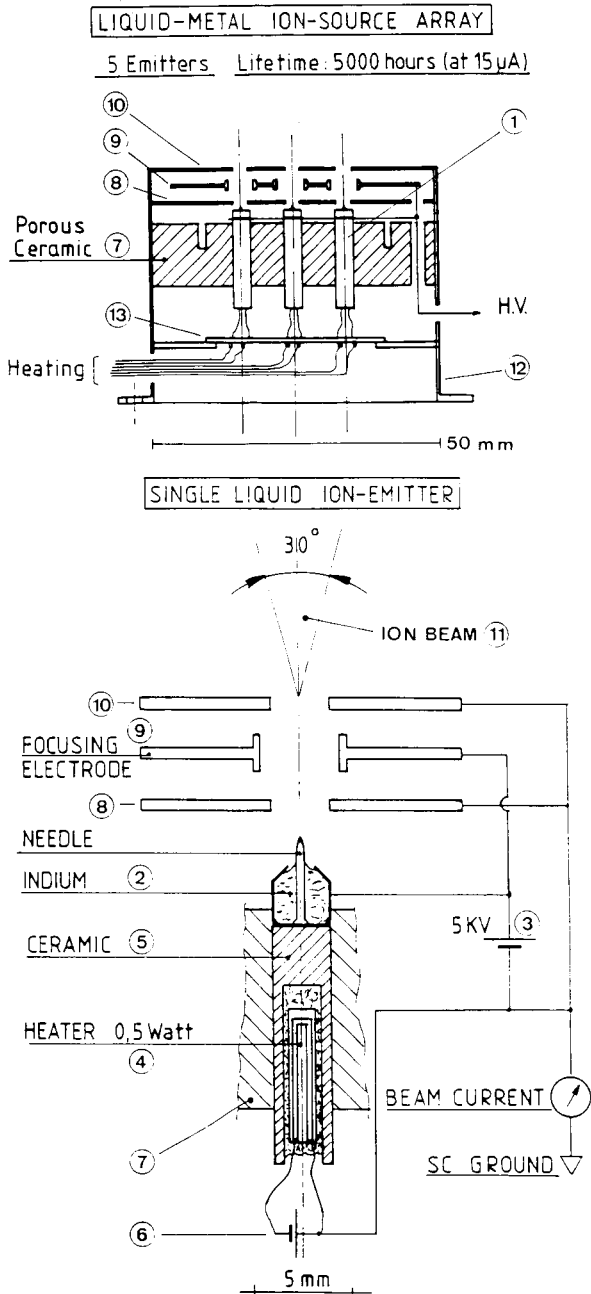


Figure 5. a) Schematic of LMIS module: (1) individual emitter, (7) thermal insulator slab, (8) extractor, (9) focusing, (10) ground electrode, (12) inner shield, (13) PCB for heater power distribution, (14) outer shield (S/C ground), (15) insulator.

b) Individual liquid metal ion emitter, see (1) in a), (2) Indium charge and needle, (3) tip power supply, (4) integrated heater, (5) ceramic insulator, (6) heater power supply, (11) outgoing In^+ beam.

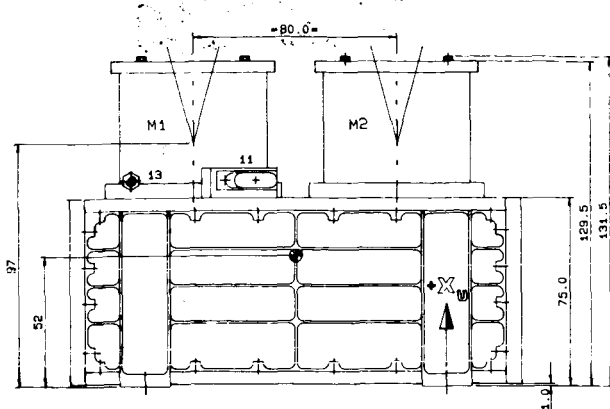


Figure 6. Mechanical drawing of the instrument.

Due to the wide-angle nonparaxial rays entering the electrode system, the lens aberrations actually will produce a finite divergence of $\pm 15^\circ$ (half maximum) in the outgoing beam (11). Note that tip and focusing electrode are on the same potential so that no additional power supply or voltage divider is required for beam focusing. Since the beam shaping and focusing optics is purely electrostatic, the lens properties and the beam shape remain unchanged if the tip voltage (identical to focusing voltage) changes.

The insulating slab and focusing system is rigidly mounted to an Aluminium support structure (12). The electrical connections to the resistive heater elements are made via 100 μm diameter Platinum wires from a printed circuit board (13), rigidly mounted to the back of the support structure.

3.2 Control Electronics

The instrument utilises a microprocessor for controlling the experiment and for data handling. It basically operates and controls the ion emitting system (high voltage and heater power), performs the start-up procedure of the emitters, and serves the interfaces to the spacecraft telemetry, the electric field and low energy electron instruments (EFW and PEACE) that have to provide S/C potential data in real-time, and the blanking pulse to the WHISPER experiment. Special attention is paid to the monitoring of the high voltage unit and the measurement of the effective ion beam current, which necessitates a special grounding concept for the emitter supply unit.

3.3 Mechanical Concept

The ASPOC instrument consists of an electronics box and two cylindrical emitter modules with 5 needles each for redundancy (M1 and M2 in Fig. 6). The emitters have to be flush-mounted with the S/C skin and with the viewing direction parallel to the spin axis to avoid spin modulation. It must be noted that the mechanical design may be changed in order to comply optimally with the requirements of the spacecraft.

4. INSTRUMENT DATA SUMMARY

The main instrument data are summarised in Table 2.

Mass

Electronics box	1080 g
2 Emitter modules	320 g
Total	1400 g

Size

Electronics box	180 × 125 × 75 mm
Emitter modules	60 mm \varnothing × 45 mm
Overall dimensions	180 × 125 × 120 mm

Power

Telemetry rate

Design life time

Emission In^+ (115 AMU) at 5 - 6 keV, < 50 μA

Beam geometry

Opening angle (half maximum)	$\pm 15^\circ$
Viewing direction	along spin axis

Table 2. Instrument Data Summary.

5. CONCLUSION

Charging of the outer surface or entire structure of a spacecraft in orbit can have a severe impact on the scientific output of the instruments. The ASPOC instrument is designed to control the surface potential of the Cluster spacecraft to near zero values for all of their operational life time. Apart from providing an improved environment, scientific investigations of the photoelectric characteristics and S/C charging can be carried out.

The instrument's small size, mass, and power consumption qualify it for the special requirements of the Cluster mission.

6. REFERENCES

1. Grard R J L 1973, Properties of the satellite photoelectron sheath derived from photoemission laboratory results, *J Geophys Res* **78**, 2885.
2. Whipple E C 1981, Potentials of surfaces in space, *Rept Prog Phys* **44**, 1197-1250.
3. Pedersen A et al 1983, Methods for keeping a conductive spacecraft near the plasma potential, *Spacecraft Plasma Interactions*, Proc 17th ESLAB Symposium, Noordwijk, The Netherlands, ESA SP-198, 185-190.

4. Knott K et al 1983, Observations of the GEOS equilibrium potential and its relation to the ambient electron energy distribution, *Spacecraft Plasma Interactions*, Proc 17th ESLAB Symposium, Noordwijk, The Netherlands, ESA SP-198, 19-24.
5. Schmidt R & Pedersen A 1987, Long-term behaviour of photo-electron emission from the electric field double probe sensors on GEOS-2, *Planet Space Sci* **35**, 61-70.
6. Lindqvist P-A 1983, The Potential of ISEE in different plasma environments, *Spacecraft Plasma Interactions*, Proc 17th ESLAB Symposium, Noordwijk, The Netherlands, ESA SP-198, 25-33.
7. Decreau P M E et al 1978, Multi-experiment determination of plasma density and temperature, *Space Sci Rev* **22**, 633-645.
8. Olsen R C 1982, The hidden ion population of the magnetosphere, *J Geophys Res* **87**, 3481-3488.
9. Olsen R C et al 1986, Aperture plane potential control for thermal ion measurements, *J Geophys Res* **91**, 3117-3129.
10. Olsen R C 1982, Field-aligned ion streams in the Earth's midnight region, *J Geophys Res* **87**, 2301-2310.
11. Grard R J L et al 1977, Comment on low energy electron measurements in the Jovian magnetosphere, *Geophys Res Lett* **4**, 247-250.
12. Scudder J D et al 1981, A survey of the plasma electron environment of Jupiter: A view from Voyager, *J Geophys Res* **86**, 8157-8179.
13. Schmidt R et al 1988, Ion emission to actively control the floating potential of a spacecraft, *Adv Space Res* **8**(1).
14. Mahoney J F et al 1969, Electrohydrodynamic ion source, *J Appl Phys* **40**, 5105.
15. Evans C A Jr & Hendricks C D 1972, An electrohydrodynamic ion source for the mass spectrometry of liquids, *Rev Sci Instrum* **43**, 1527.
16. Wagner A & Hall T M 1979, Liquid gold ion source, *J Vac Sci Tech* **16**, 1871.
17. Dixon A J & von Engel A 1980, Studies of field emission gallium ion sources, *Inst Phys Conf Ser* **54**, 292.
18. Taylor G I 1964, Disintegration of water drops in an electric field, *Proc Royal Soc (London)* **A280**, 383.
19. Kingham D R & Swanson L W 1984, Mechanics of ion formation in liquid metal ion sources, *Appl Phys* **A34**, 123.
20. Kubena R L et al 1981, GaAs MESFET fabrication using maskless ion implantation, *IEEE Electron Dev Lett*, **EDL2**, 152.
21. Seliger R L et al 1979, High-resolution, ion-beam processes for microstructure fabrication, *J Vac Sci Tech* **16**, 1610.
22. Rüdener F G 1984, Liquid metal ion sources for scanning SIMS, *Secondary Ion Mass Spectrometry; SIMS IV*, Eds Benninghoven A et al, Springer Verlag, Berlin, 133.
23. Bartoli C H et al 1982, Liquid metal ion sources for space propulsion, *Proc 29th Int Field Emission Symposium*, Eds Andren H O & Norden H, Almqvist & Wiksell, Stockholm, 363.
24. Rüdener F G et al 1987, *Int J Mass Spectrom Ion Proc*, in press.